Supporting Information

DNA-inorganic hybrid nanovaccine for cancer immunotherapy

Guizhi Zhu[a], Yijing Liu[a], Xiangyu Yang[a], Young-Hwa Kim[a], Huimin Zhang[a], Rui Jia[b], Hsien-Shun Liao[c], Albert Jin[c], Jing Lin[c], Maria Aronova[c], Richard Leapman[c], Zhihong Nie[d], Gang Niu[a], and Xiaoyuan Chen[a,*]

[a] Laboratory of Molecular Imaging and Nanomedicine, National Institute of Biomedical Imaging and Bioengineering (NIBIB), National Institutes of Health (NIH), Bethesda, MD 20892

[b] Section on Intracellular Protein Trafficking, Cell Biology and Metabolism Program, National Institute of Child Health and Human Development, NIH, Bethesda, MD 20892

[c] Laboratory of Cellular Imaging and Macromolecular Biophysics, NIBIB, NIH, Bethesda, MD 20892

[d] Department of Chemistry and Biochemistry, University of Maryland, College Park, MD 20742

[*] Corresponding Author: shawn.chen@nih.gov; (+1) 301-451-4246

Supplemental Experimental Section

Synthesis of DNA. DNA was synthesized on an ABI 392 DNA synthesizer (Applied Biosystems) on a 1 μmole scale using solid phase synthesis. Phosphoramidites and related reagents used for DNA synthesis were purchased from Glen Research (Sterling, VA) or Chemgenes (Wilmington, MA). Phosphothiolate (PS) CpG or GpC was synthesized by replacing Sulfurizing Agent (Glen Research, Sterling, VA) in place of iodine oxidation reagent. DNA was deprotected by incubating in methylamine and ammonium oxide (1:1) solution, unless otherwise noted, at 65 ^{o}C for 30 min. DNA was purified using reverse phase HPLC on a Dionex Ultimate 3000 (ThermoFisher Scientific, Waltham, MA) using C18 column and lyophilized. DNA was further treated with acetic acid (0.5 M) to remove the dimethoxytrityl (DMT) protecting group, desalted, and quantified on a Genesys 10S UV-Vis spectrometer (ThermoFisher Scientific, Waltham, MA).

Cell lines and cell culture. RAW264.7 macrophage cell and B16F10 cell were obtained from ATCC, cultured in DMEM medium supplemented with heat-inactivated FBS (10%), 100 U/mL penicillin, and 100 μg/mL streptomycin, in a cell culture incubator with 5% CO_2 at 37 °C.

Cytotoxicity assay. The cytotoxicity of hNVs was evaluated using an Alamar Blue assay (ThermoFisher Scientific, Waltham, MA). Particularly, 1 x 10^4 B16F10 cells were seeded into each well in a 96-well plate, and one day afterwards, cells were treated with hNVs at a series of specified concentrations. 2 days after treatment, cells were treated with Alamar Blue reagent, and the absorbance of cell solution was read on a BioTek plate reader (Winooski, VT) (Ex: 580 nm; Em: 590 nm). Cell viability was calculated as per manufacturer's instructions.

Evaluation of the stability of hNVs. The stability of hNVs under nuclease cleavage was evaluated by treating hNVs with DNase I (5 U/mL, 37 °C; New England Biolabs, Ipswich, MA) for 1 h, followed by nuclease deactivation at 75 °C for 10 min. The stability of hNVs against thermal denaturation was performed by heating hNVs at specified temperature for 1 h. The morphologies of the resultant hNVs were examined using SEM as described above.

Quantification of DNA yield of RCR. hNVs were treated with EDTA (5 mM), which chelated Mg^{2+} and led to dissolution of hNVs. DNA was purified by removing EDTA, Mg^{2+}, and PPi^{4-} using centrifugation filtering (Millipore Ltd., Billerica, MA). The absorbance of the resulting DNA was determined on a Genesys 10S UV-Vis spectrometer (ThermoFisher Scientific, Waltham, MA) and converted to the equivalent of CpG for the estimation of DNA yield.

In vitro **cell uptake of hNVs.** *In vitro* cell uptake of nanovaccines was studied using confocal laser scanning microscopy and flow cytometry. Alexa488-labeled nanovaccines were incubated with RAW264.7 cells or BMDCs for 4 h, and stained with Lysotracker Red DND-99 (Life Technologies, Carlsbad, CA) and 10 μg/mL Hoechst33342 (Life Technologies, Carlsbad, CA) for 0.5 h in a cell culture incubator at 37 °C before confocal observation. Cells were then

washed with Dulbecco's PBS for three times before imaging on a Zeiss LSM 780 confocal microscope (Chesterfield, VA). Alternatively, flow cytometry was used to study the cell uptake using a BD Beckman Coulter flow cytometer (Brea, CA) or BD Accuri C6 flow cytometer (San Jose, CA). For flow cytometric analysis, RAW264.7 cells or BMDC cells were seeded into 24-well plate, and one day later, cells were treated with Alexa488-labeled hNVs for 4 h, following by detaching cells using non-enzymatic dissociation buffer (Invitrogen, Grand Island, NY), washing with Dulbecco's PBS for three times, and flow cytometric analysis of Alexa488 fluorescence intensities of cells.

Supplemental Figures

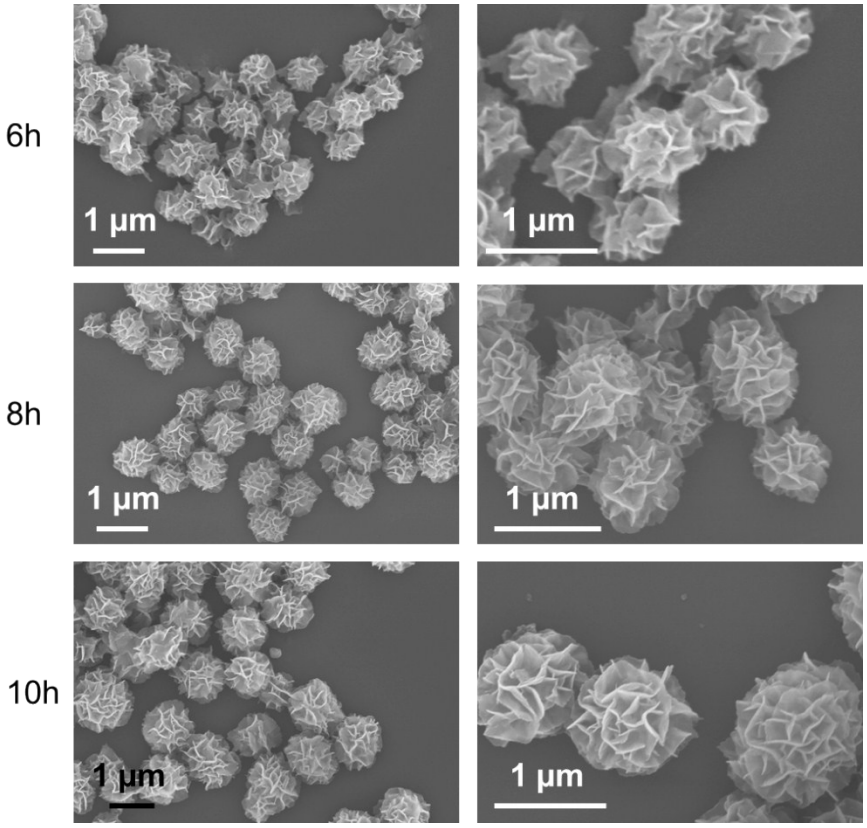

Fig. S1. SEM images showing that the sizes of hNVs can be tuned by simply controlling the RCR reaction time.

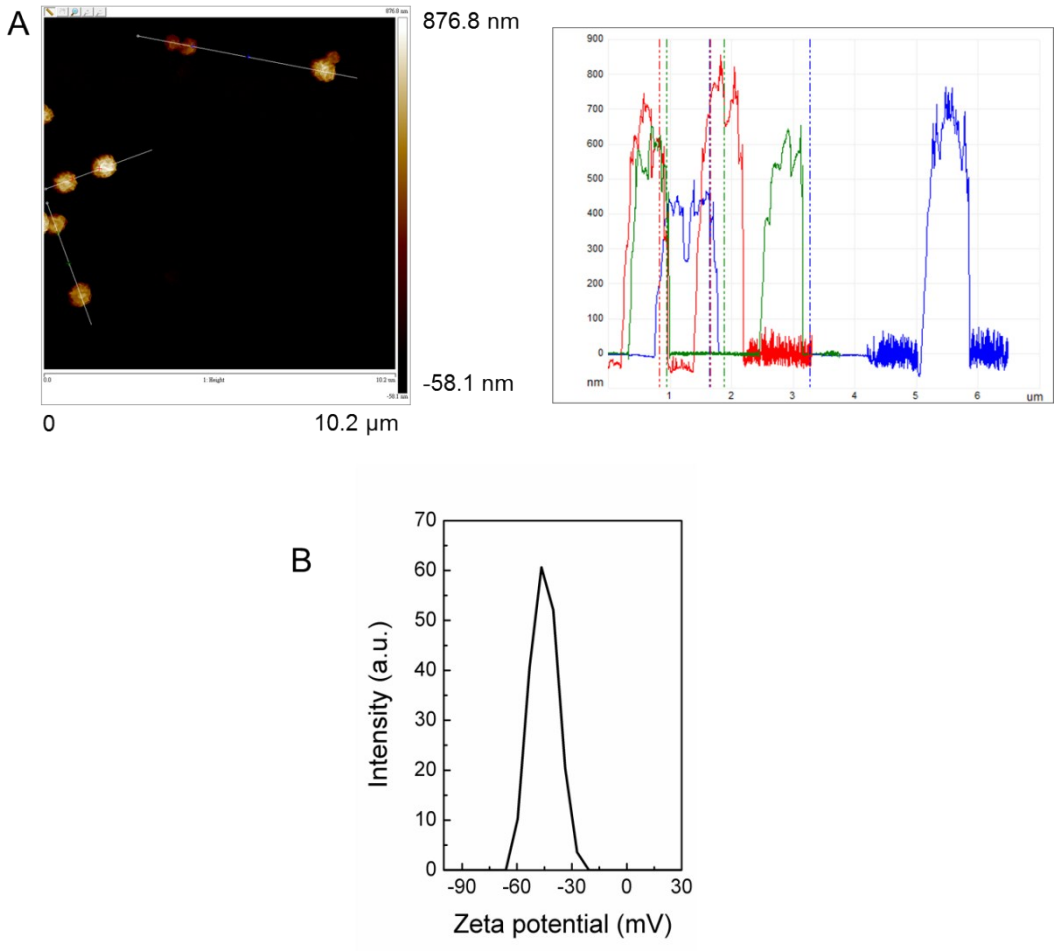

Fig. S2. (A) AFM images (left) and the corresponding dimension measurement results (right) of hNVs. The red lines in AFM images marked the location of dimension measurement. (B) Zeta potential of hNVs was determined to be -45 mV.

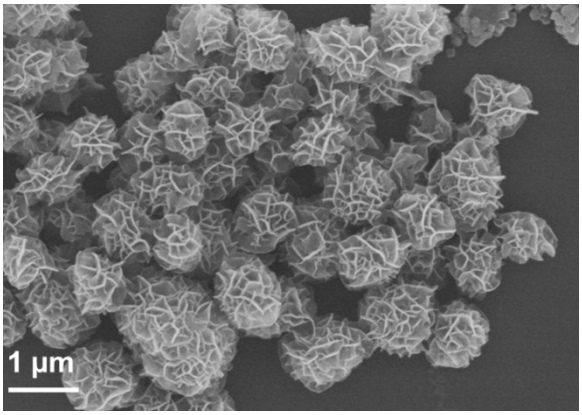

Fig. S3. An SEM image showing that GpC-inorganic hybrid nanoflowers self-assembled by RCR using a template that was mutated to encode GpC, in place of CpG in hNVs. GpC-inorganic hybrid nanoflowers were utilized as the control of hNVs.

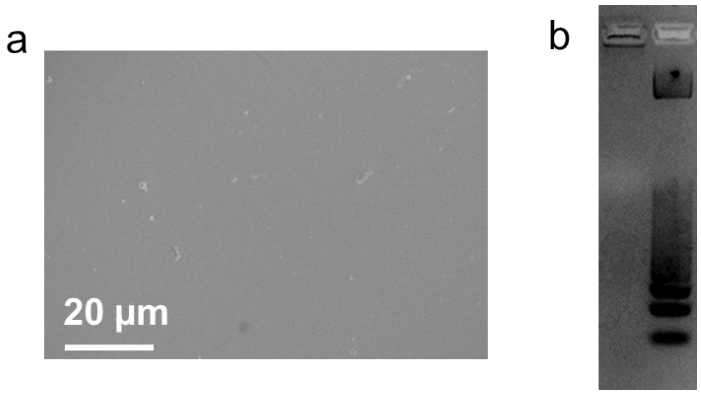

Fig. S4. Dissolution of hNVs by treatment with EDTA. (*A*) An SEM image showing that hNVs were dissolved by treating with EDTA (5 mM) for 30 min. The remaining DNA molecules were visible by SEM. (*B*) An image of agarose gel electrophoresis of the remnant DNA from EDTA-treated hNVs. The hNV DNA stayed in the gel well, likely due to the large sizes and the intermolecular complexation. (Left lane: sample DNA; right lane: 25 bp DNA ladder)

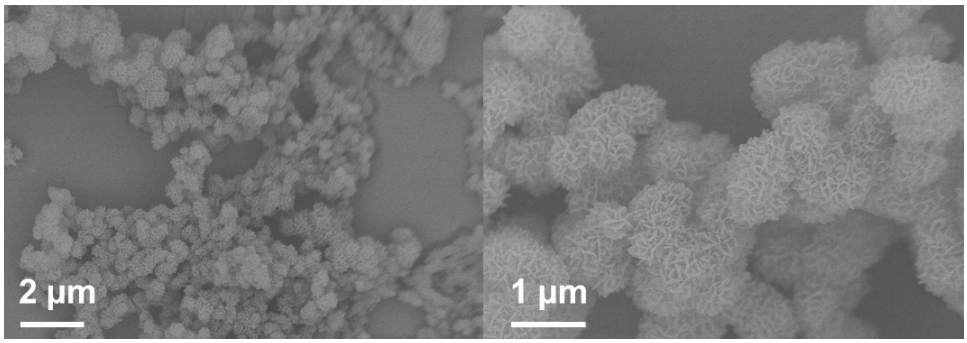

Fig. S5. SEM images showing pure Mg_2PPi nanostructures, which were formed by simply mixing Mg^{2+} (16 mM) with PPi^{4-} (5 mM). The morphology of Mg_2PPi nanostructures simulated that of hNVs.

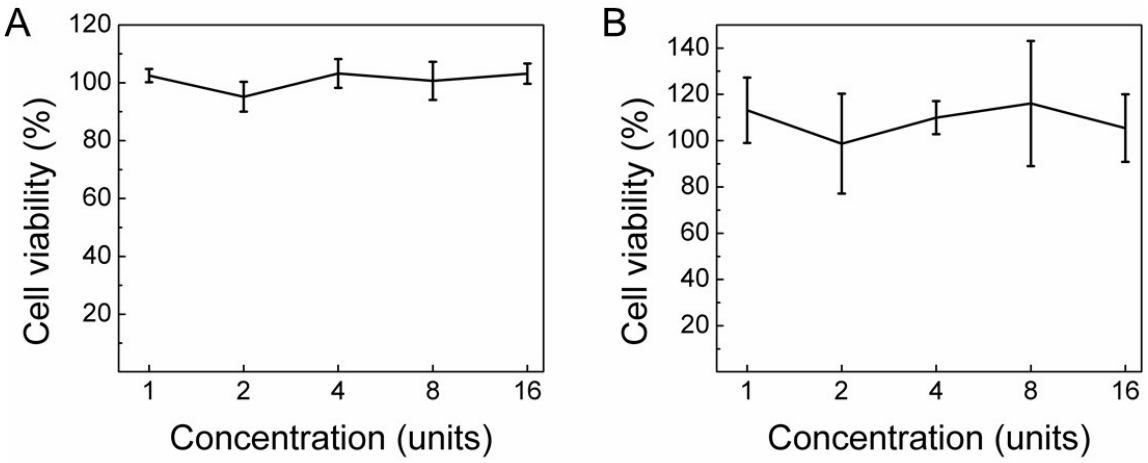

Fig. S6. Alamar Blue assay results showing negligible cytotoxicity of hNVs in B16F10 melanoma cells (A) and macrophage-like RAW264.7 cells (B). 1 unit of hNVs is equivalent to 10 nM CpG.

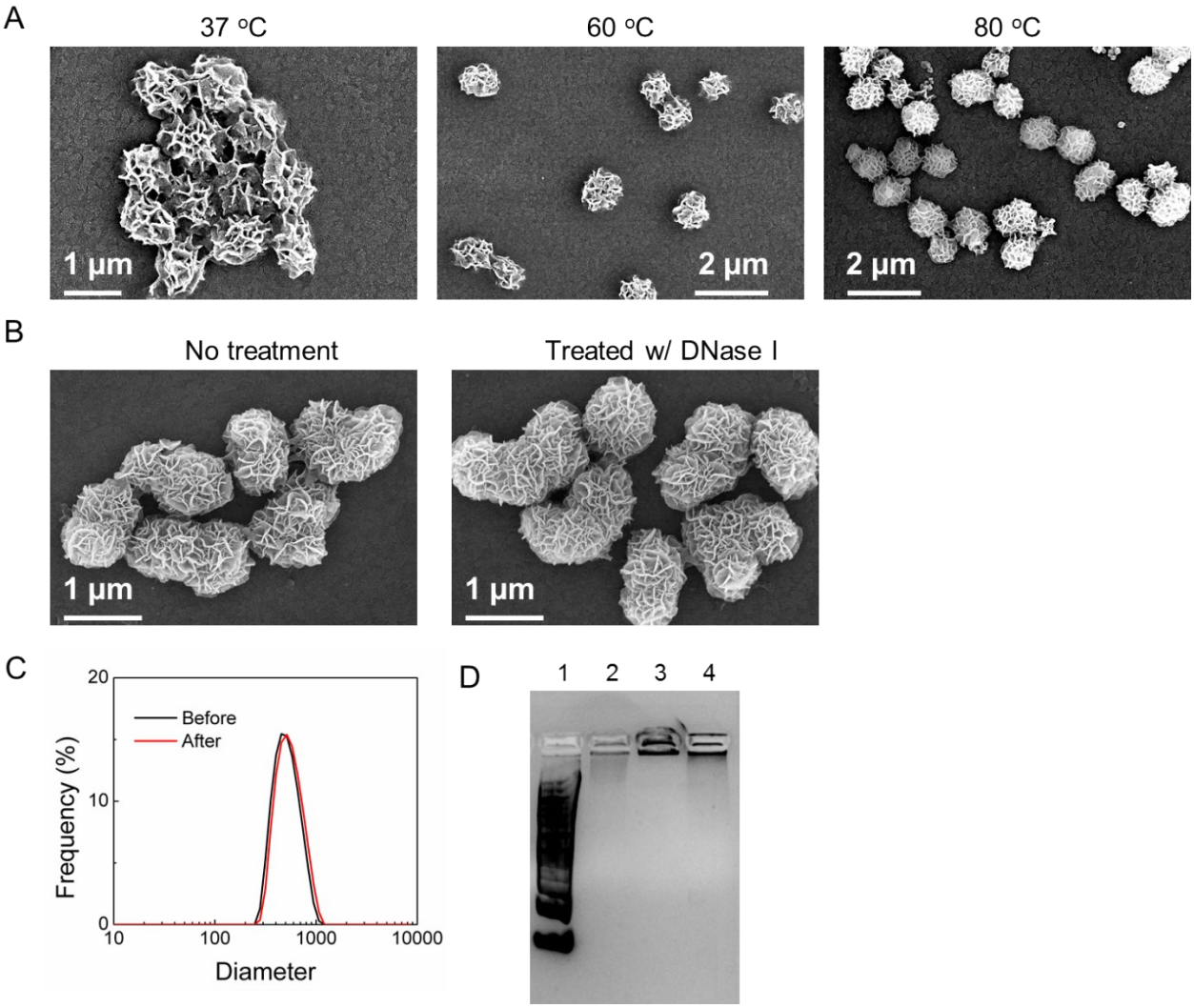

Fig. S7. High stability of hNVs as dry powder, under high temperature, and in mimicked physiological conditions. (*A*) SEM images showing the intact hNV structures after heating hNVs at the indicated temperature as dry powders. (*B*) SEM images showing the intact hNV structures after incubating hNVs under the treatment with DNase I (5 U/mL), which was used to mimic the interstitial fluid that vaccines are often exposed to. (C) DLS results demonstrating that the sizes and dispersion of hNVs were not significantly changed after incubation in physiological buffer for one day. (D) An image of agarose electrophoresis showing that DNA in hNVs was released from hNVs upon incubation at pH5 for 2h, and that the DNA in hNVs maintained the integrity after incubating hNVs in serum (50%) for 2h. Sample legends: 1, 100 bp DNA ladder; 2, hNVs incubated at pH5; 3, hNVs in PBS; 4, serum-treated hNVs. All hNVs were treated with EDTA for 1h before gel electrophoresis.

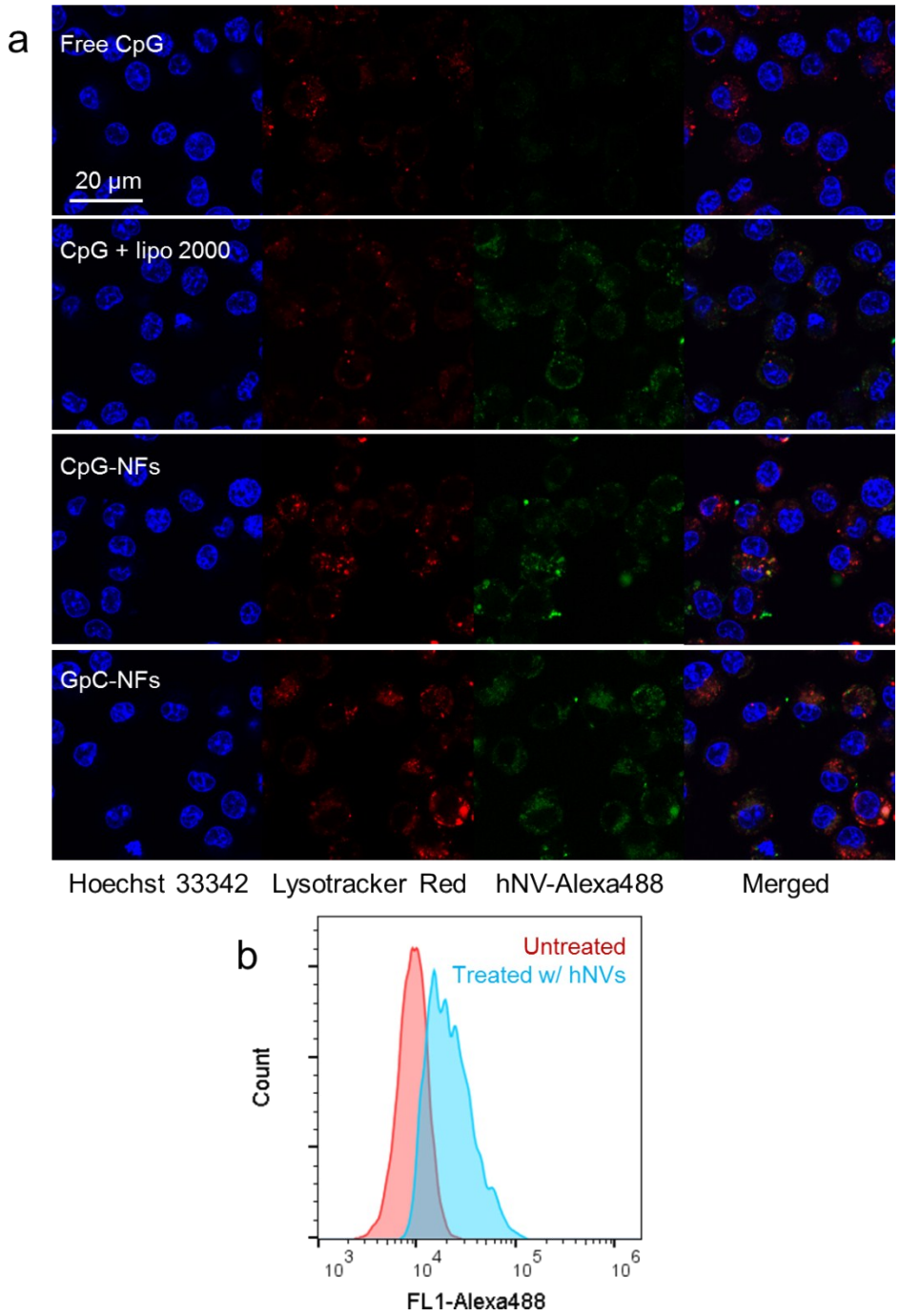

Fig. S8. Efficient uptake of hNVs into macrophage-like RAW264.7 cells. (*A*) Confocal microscopy images displaying that Alexa488-labeled hNVs were localized inside RAW264.7 cells after incubation for 4 h, and that Alexa488-labeled hNVs were colocalized with the endolysosome. Endolysosome was stained by Lysotracker Red DND-99. (*B*) Flow cytometric analysis of RAW264.7 cells incubated with Alexa488-labeled hNVs for 4 h.

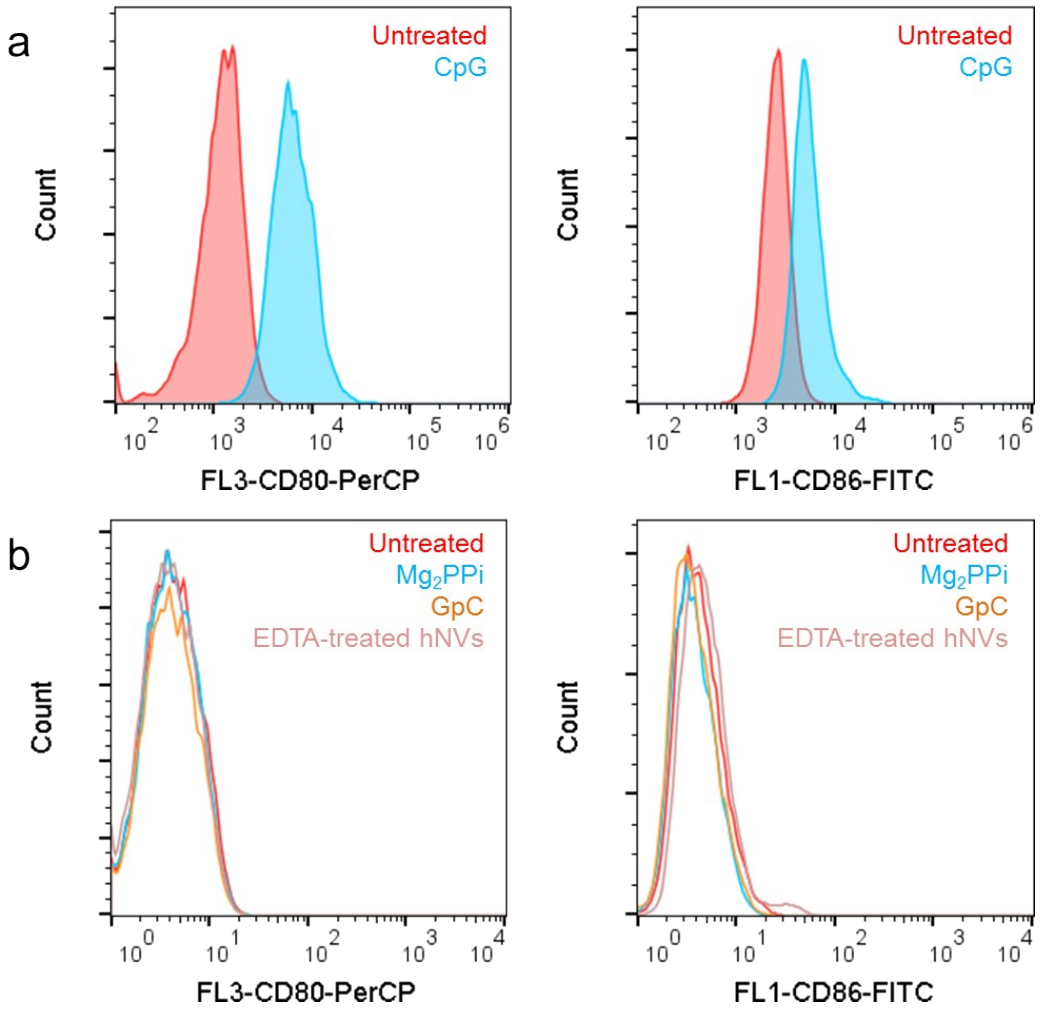

Fig. S9. Flow cytometry results showing that the expression of costimulatory factors CD80 and CD86 were (*A*) elevated in RAW264.7 cells treated with molecular CpG, but (*B*) negligibly elevated in RAW264.7 cells treated with control GpC-NFs, Mg_2PPi nanostructures, or hNVs treated with EDTA, at the concentrations of 100 nM equivalent CpG for 24 h.

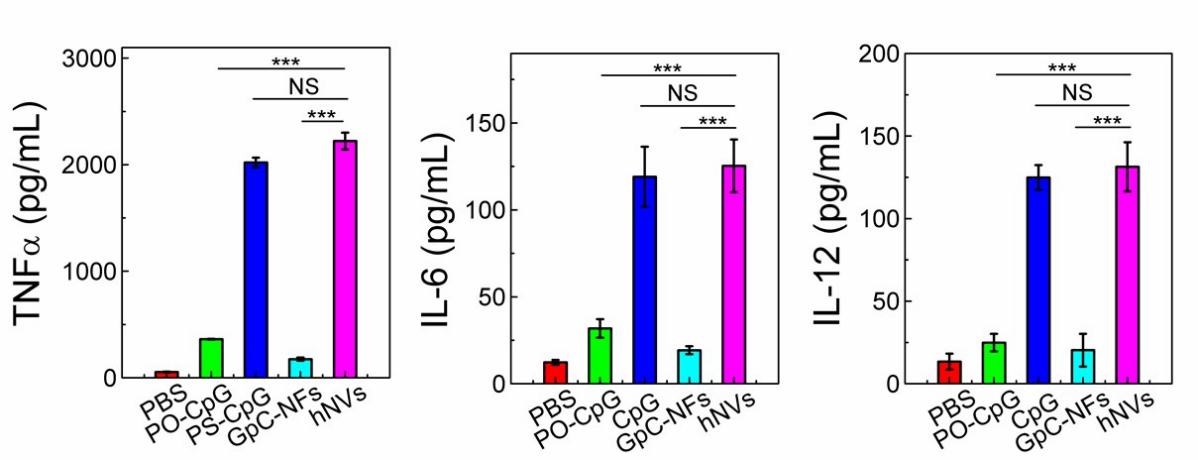

Fig. S10. ELISA results suggest hNVs and PS-CpG induced RAW264.7 cells to secret significantly more proinflammatory cytokines TNFα, IL-6, and IL-12, than parent PO-CpG. Experiment conditions were the same as that in Fig. 3*B*. Asterisks represent significant differences between cells treated with the corresponding different regimes (***$p<0.001$, *$p<0.1$; n = 3; one-way ANOVA with Bonferroni post test). Data represent mean ± s.d. NS, not significant.

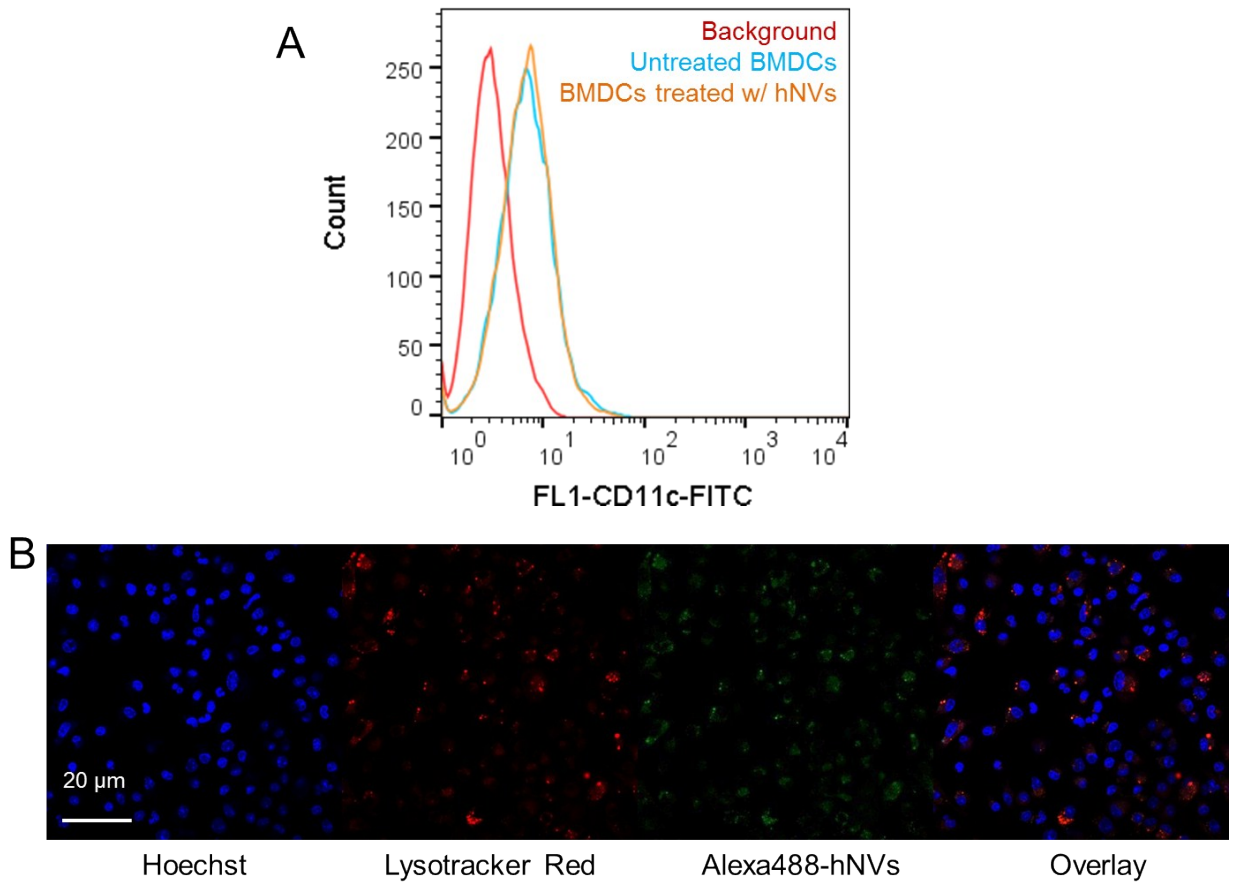

Fig. S11. (*A*) Flow cytometric analysis of BMDCs showing the expression of CD11c, a DC marker. BMDCs treated with hNVs (100 nM CpG equivalent) maintained expression of CD11c. (*B*) Confocal microscopy images displaying that Alexa488-labeled DNA in hNVs was localized inside BMDCs after incubation for 4 h. The endolysosome was stained by Lysotracker Red DND-99.

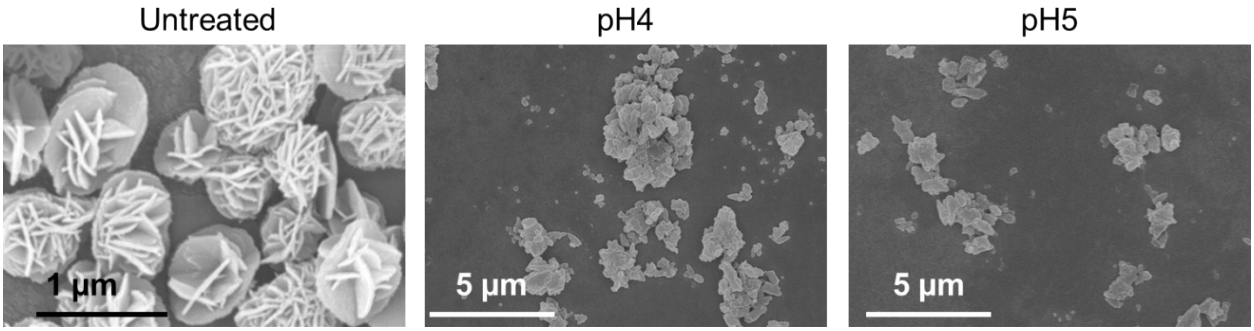

Fig. S12. SEM images showing that hNVs were dissovled in endolysosome-mimicking acidic environment for 1 h.

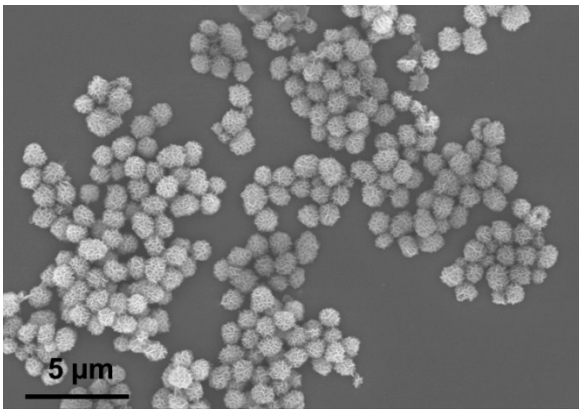

Fig. S13. An SEM image showing IR800-labeled hNVs.

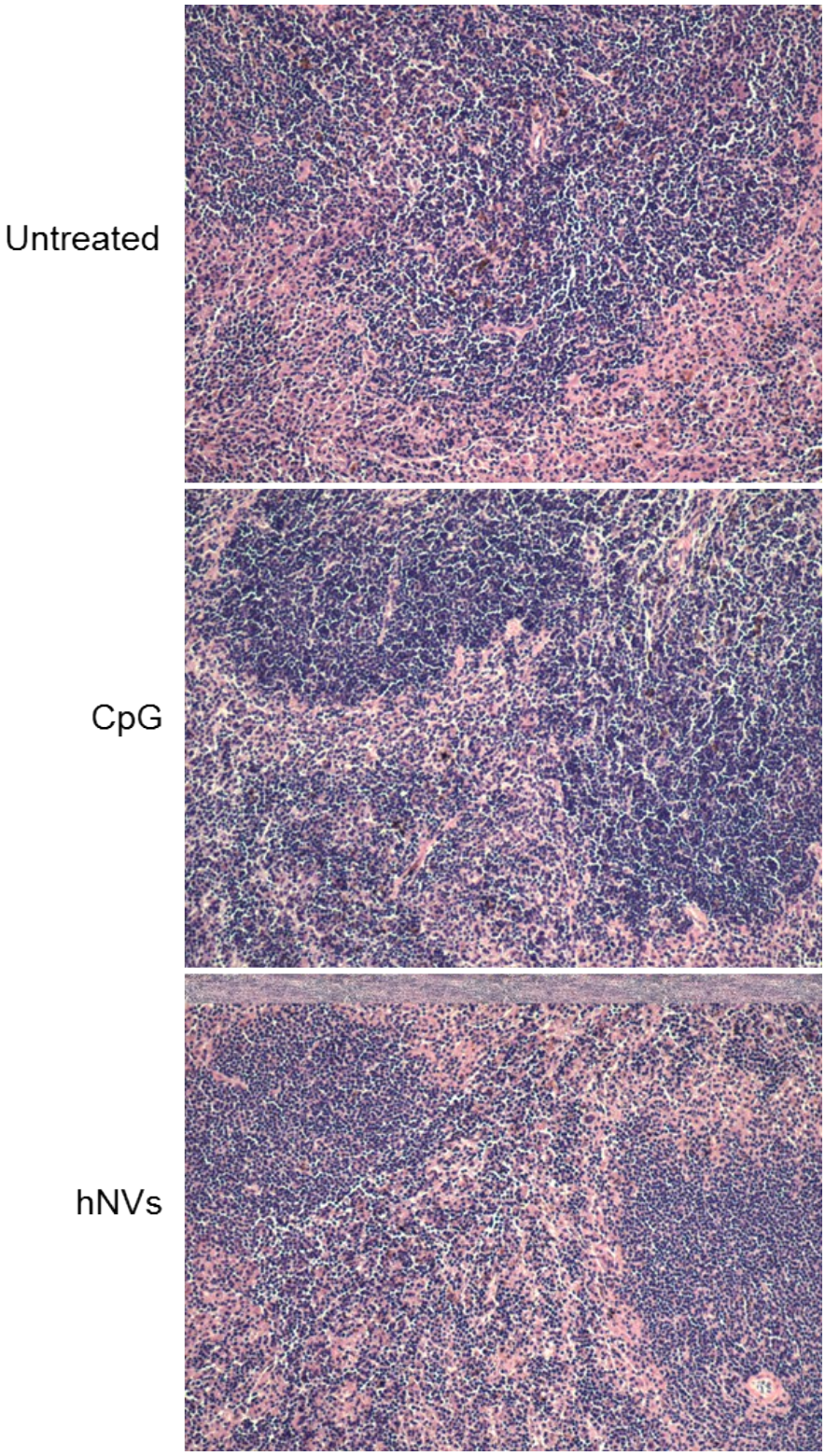

Fig. S14. Representative images of the H&E staining of spleens after mice were treated with PBS, molecular CpG, or hNVs.

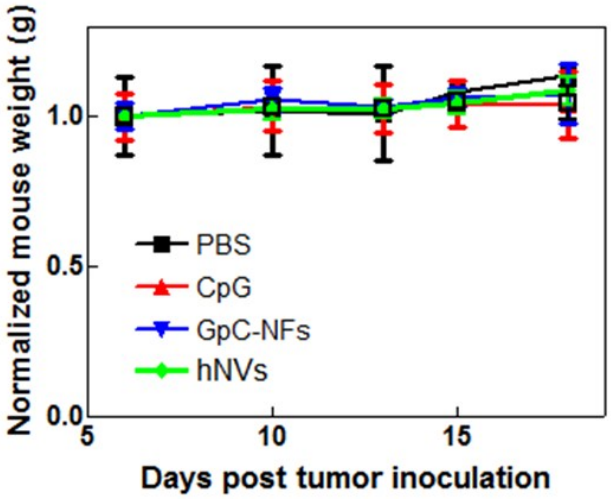

Fig. S15. Mouse weights monitored during the course of treatment. No significant weight loss was observed in mice treated with hNVs or other regimes.

Supplemental Tables

Table S1. DNA sequences. CpG (CpG 1826) had phosphothioate backbone unless denoted otherwise, and all other DNA had phosphodiester backbone. Purple sequences: CpG or CpG analogs; Red sequences: GpC or GpC analogs; Underlined sequence: complementary sequences between primers and the corresponding templates; Shaded sequence: CpG or GpC dinucleotide.

	Sequences (5'-3')
CpG	TCCATGACGTTCCTGACGTT
GpC	TCCATGAGCTTCCTGAGCTT
Primer for hNVs	ACGTTCCTGACGTTTTTCAGCGTGACTTTTCCATGACGTTCC
Template for hNVs	CGCTGAAAAACGTCAGGAACGTCATGGAAAAAAAACGTCAGGA ACGTCATGGAAAAAAAACGTCAGGAACGTCATGGAAAAGTCA
Primer for GpC-NFs	AGCTTCCTGAGCTTTTTCAGCGTGACTTTTCCATGAGCTTCC
Template for GpC-NFs	CGCTGAAAAAGCTCAGGAAGCTCATGGAAAAAAAAGCTCAGGA AGCTCATGGAAAAAAAAGCTCAGGAAGCTCATGGAAAAGTCA